Metastable transformation states of decagonal Al-Co-Ni due to inhibited decomposition

M. Döblinger and R. Wittmann*
Laboratorium für Elektronenmikroskopie, Universiät Karlsruhe, Kaiserstr. 12, D-76128 Karlsruhe, Germany

B. Grushko
Institut für Festkörperforschung, Forschungszentrum Jülich, D-52425 Jülich, Germany
(Received 14 March 2001; published 12 September 2001)

The transformation behavior of high-Co decagonal Al-Co-Ni is studied. Starting from stability considerations based on a number of annealing treatments we check theoretical predictions of the stabilization mechanism and transformation mechanism by phason strain analysis and tiling analysis. The quasicrystal transforms in the first stages into nanodomain structures and finally decomposes into a quasicrystal and a normal crystalline phase. Before decomposition, the material is locked in a disordered state exceeding the periodic order allowed for a one-dimensional quasicrystal. This is interpreted as the maximum periodic order achievable without diffusion. From considering different reasons for phason strain we conclude that disorder in tilings related to phase transformations can wrongly be associated with that suggested by the random tiling hypothesis.

DOI: 10.1103/PhysRevB.64.134208 PACS number(s): 61.44.Br, 61.50.Ks, 68.37.Lp

I. INTRODUCTION

The Al-Ni-Co alloy system is known to contain a number of modifications of the decagonal (D) quasicrystalline structure[1–7] as well as a number of closely related periodic pseudodecagonal structures (approximants).[4,7–9] These phases are formed in a wide compositional range along about $Al_{73}Co_{27}$-$Al_{69}Ni_{31}$.[4,6,7] In addition, at compositions in the middle of this range, low-temperature nanodomain structures (NDS's) are observed where small periodic domains are mutually oriented, which results in an overall ''almost'' decagonal symmetry.[10,11] Quasicrystals are typically observed in as-cast materials and in material annealed just below the melting temperature, while approximants of the same compositions appear after annealing 100 K to 200 K below the melting temperatures.[9] Although up to eight quasicrystalline modifications are reported to be thermodynamically stable[7] this was not confirmed for any of the low-temperature approximants.[9,12]

For the low-temperature quasicrystals in the Al-Co-Ni system the arrangement of building units, used as vertices to construct a tiling, was described to be random.[13,14] On the other hand, this was not observed for the high-temperature phase, the basic decagonal phase.[13] A random arrangement of vertices is usually linked to an entropic stabilization due to the tiling arrangement, referring to the theory known as random tiling hypothesis.[15–17] Stacking disorder in the periodic direction required for such an entropic stabilization was also observed for decagonal quasicrystals in the Al-Ni-Co system.[18] However, a random tiling stabilization was rather expected for high-temperature phases as opposed to for low-temperature phases. In this context, a stabilization mechanism based on chemical disorder was suggested for the basic decagonal phase.[13]

The basic decagonal phase is obtained at room temperature at extremely low Co concentrations[4] only. *In situ* x-ray measurements[5] have shown that the corresponding diffraction pattern appears along the whole stability range of the decagonal phase up to high Co concentrations as a high temperature phase. The numerous modifications of the decagonal phase are usually described using the concept of the structure of the basic decagonal phase and its different superstructures. The ''Edagawa type'' superstructures[8] (S1 superstructure and S2 superstructure) can be derived in a higher-dimensional description with a five times enlarged unit cell with respect to the basic decagonal phase.[19,20]

Another diffraction pattern was observed by Grushko and Urban[3] and studied in more detail by Ritsch *et al.*,[21] where it was called ''superstructure type II'' (SST-II). It was observed in the central part of the homogeneity region of the decagonal phase and is reported to be a stable quasicrystal transforming from the S1 superstructure below about 1170 K. The superstructure reflections were observed to be in the middle between basic reflections. A description of SST-II based on color symmetry was suggested by Scheffer.[22]

The existence of a C-centered one-dimensional quasicrystal (1D QC) with a 6.1 nm period in the system Al-Ni-Co was suspected by Edagawa *et al.*[23] and shown to exist in a NDS by Kalning *et al.*[11] Its stability was reported by Ritsch *et al.*[24] for compositions around $Al_{71}Co_{18-22}Ni_{11-7}$ above 1170 K. NDS's in Al-Co-Ni were studied in samples of $Al_{70}Co_{15}Ni_{15}$ nominal composition. The periodic arrangement of reflections in NDS's indicate that they can be composed of multiply twinned 1D QC's or multiply twinned approximants. There are arguments in favor of a close relationship between SST-II and NDS. A phason-strain-based description of SST-II was given recently by Weidner *et al.*[25] Due to the slope of the solidus and the liquidus line, the material of nominal $Al_{70}Co_{15}Ni_{15}$ prepared by cooling slowly can contain considerable amounts of more Co-rich material corresponding to the reported stability region of SST-II. However, high-resolution transmission electron microscopy (HRTEM) on SST-II[21] revealed that there is no obviously visible periodicity. This can be taken as a strong argument in favor of the quasicrystalline nature of SST-II. NDS's are regarded to play an important role in the transformation from quasicrystals to approximants.[26,27] However, they were ob-

served to be rather stable at least in a kinetical sense[28] in the system Al-Cu-Co(Si), which is closely related to Al-Co-Ni.

To study the transformation behavior of the decagonal phase at low temperatures a composition belonging to the region associated with SST-II was selected. By this means, we expected to elucidate possible relationships between SST-II and NDS. In this context we also wanted to focus on possible transition states between the structures appearing at this composition.

II. EXPERIMENTAL METHODS

In our work the samples are first studied by scanning electron microscopy and powder x-ray diffractometry, then by electron diffraction using larger and smaller apertures and by high-resolution electron microscopy. The sequence of the methods applied for the materials annealed for increasing times allows us to monitor the transitions starting from the coarse scale to more and more fine scale. The investigation of the long-term annealed material by coarser methods provides the basis for the interpretation of the high-resolution patterns obtained from the shorter-term annealed material where the changes are not yet developed. The latter, in turn, supply important information on the transformation trends.

Ingots of nominal composition of $Al_{72.5}Co_{15.5}Ni_{12}$ were prepared by inductive melting in a water-cooled copper crucible under an Ar atmosphere. The material was homogenized for 43 h at 1290 K, which is just below the solidus for this composition. Both this preannealed and as-cast materials were additionally annealed at 1140 K in evacuated silica ampules for 384 h, 1125 h, and 2718 h. The long annealing durations are chosen because of a sluggish transformation behavior[9] in this system. The samples were examined metallographically and by powder x-ray diffraction (Stoe diffractometer using Co $K\alpha$ radiation in transmission mode) prior to detailed investigations by HRTEM and electron diffraction. Microprobe analysis (Cameca camebax SX 50) was used to check the local phase compositions and their fluctuations. HRTEM and electron diffraction were carried out with a Philips CM 200 ST/FEG ($C_s = 1.2$ mm) microscope operating at 200 kV on powdered specimens supported on carbon nets.

III. METALLOGRAPHY AND X-RAY DIFFRACTION

Metallographic examinations of the material annealed at 1290 K confirmed its single-phase constitution and compositional homogeneity. The maximum compositional fluctuations were below 0.3 at. %. The powder x-ray diffraction pattern was typical of the decagonal phase.[3] Similar results were obtained for the preannealed material, which was additionally annealed at 1140 K for 384 h and 1125 h. In the latter a small quantity of a crystalline phase was observed by transmission electron microscopy. In contrast, the parts that were additionally annealed at 1140 K for 2718 h exhibited two-phase constitution. Powder x-ray diffractometry confirmed here the existence of the C-centered monoclinic *X* phase[4,7] and the decagonal phase. The average compositions of all the samples were close to $Al_{71.9}Co_{15.4}Ni_{12.7}$ with fluctuations of less than 0.5 at. %. No systematic shift of the composition with the annealing duration was revealed. This allows us to conclude that for the studied composition at 1290 K a homogeneous decagonal phase transforms at 1140 K to a mixture of a decagonal phase plus the *X* phase during 2718 h while for a shorter annealing some intermediate states occur. This is corroborated by the fact that the *X* phase cannot be solidified from the melt.[29] In samples that were not preannealed the formation of the *X* phase was also observed after annealing at 1140 K for 2718 h.

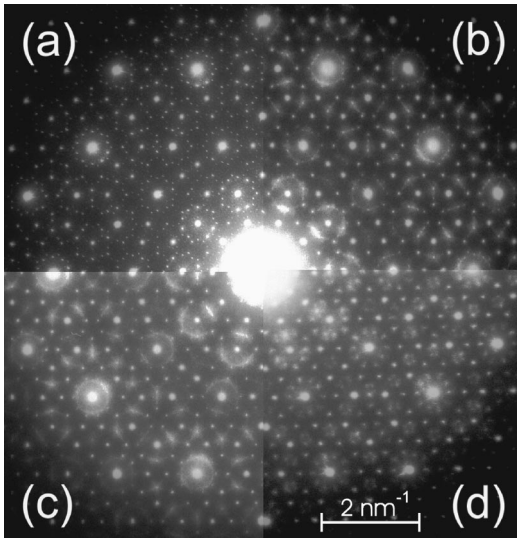

FIG. 1. (a) Diffraction pattern of the S1 phase originating from preannealed material; (b)–(d) diffraction patterns of different ordering states observed after annealing preannealed material for 384 h at 1140 K.

IV. ELECTRON DIFFRACTION

TEM investigation of the samples annealed for 2718 h at 1140 K from the as-cast state confirmed the formation of the *X* phase. The second structure, an approximant, is so-called PD1.[9] As will be shown below, PD1 was never observed in the samples procedured under the same conditions but preannealed. In the following we concentrate only on the study of the preannealed samples.

In material that was annealed at 1290 K for 43 h only the S1 superstructure was observed. The diffraction pattern along the tenfold axis of this decagonal superstructure is shown in Fig. 1(a). Peak shifts were not observed within the accuracy of image formation. Although powder x-ray diffraction of the samples annealed at 1140 K for 384 h did not reveal any changes as compared to the preannealed material, the corresponding electron diffraction indicates a series of closely related structures with an overall decagonal symmetry. They fit into a sequence of diffraction patterns where the superstructure reflections of the S1 phase become diffuse and finally vanish while diffuse reflections, located roughly in the middle between two reflections of the basic decagonal phase, appear. Therefore these structures can be interpreted as intermediate states between the S1 superstructure and SST-II.

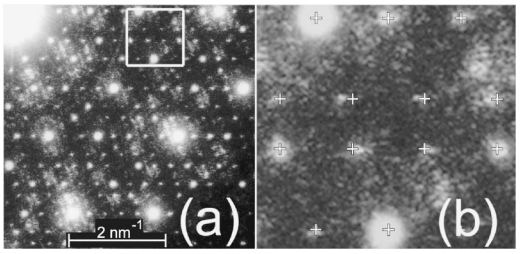

FIG. 2. (a) Diffraction pattern of the same region as in Fig. 1(d) but taken with a smaller aperture. (b) Magnified detail of diffraction pattern (a) for comparison with theoretical reflection positions of a 1D QC. The positions of the weak reflections in the center of the image show considerable deviations from a 1D QC.

Typical diffraction patterns of these states are shown in Figs. 1(b)–1(d).

The diffraction pattern on Fig. 1(d) taken with an aperture of 760 nm in diameter shows the typical features of SST-II (Ritsch *et al.*,[21] Fig. 2). Using an aperture of only 170 nm in diameter for the same region reveals a completely different diffraction pattern. It shows that the structure represented in diffraction pattern of Fig. 1(d) is built of small fivefold twinned domains. The diffraction pattern of one of these domains is represented in Fig. 2(a). Splitting of reflections is not observed here in the limits of resolution, reflecting that there is one predominant domain orientation. In the first approximation, it is periodic in the horizontal direction suggesting a 1D QC with a period of 3.05 nm (6.1 nm with centering). Tilted by 72° to the periodic direction, very weak diffuse streaks can be recognized in the vicinity of strong reflections. Their distances agree with a period of 3.05 nm. A comparison of the observed diffraction pattern with the peak positions of a simulated diffraction pattern of a 1D QC with $a=6.1$ nm is shown in Fig. 2(b). The peak positions are shifted from expected positions for a 1D QC along the horizontal direction (see Sec. V). This indicates that the transition from the decagonal S1 superstructure to a 1D QC is incomplete.

In order to check if the quasicrystal transforms at lower temperatures to normal-crystalline phases another annealing treatment was performed. The preannealed material was annealed for 240 h at 1110 K instead of 1140 K. As in the previous sample we observed only transition states between the S1 superstructure and the 1D QC. The slow transformation kinetics from the S1 superstructure to SST-II could be confirmed this way.

The material annealed at 1140 K for 1125 h typically shows diffraction patterns of SST-II besides a minor crystalline phase (less than 5%). S1 reflections are not observed any longer but the decagonal-like diffraction patterns are still not identical. This indicates that the transition is not finished yet. In Fig. 3(a) the main reflections are clearly split and reflections typical for SST-II are quite sharp while in Fig. 3(b) the main reflections are broadened and reflections typical for SST-II are blurred. This indicates different coherence lengths. Again, using a small aperture we see that the diffraction patterns are composed of twinned nanodomains. Figure

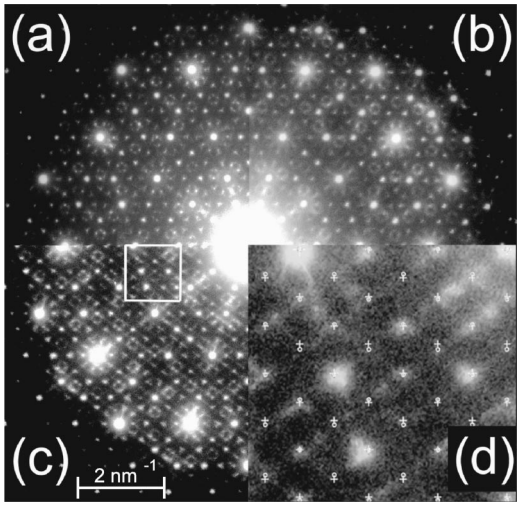

FIG. 3. Diffraction patterns of material annealed for 1125 h at 1140 K after preannealing. Diffraction pattern (a) shows sharp or clearly split reflections. The reflections in (b) are, in comparison, blurred and broadened. (c) Diffraction pattern exhibiting intense streaks arranged according to a lattice of $a=b=5.18$ nm, $\gamma=108°$ taken with a small aperture. (d) Magnified detail of (c). For comparison reflection positions of the (4,6) approximant (circles) and 1D QC (crosses) are shown.

3(c) shows a typical diffraction pattern with one predominating domain orientation being smaller than the aperture. This can be inferred from the triangular shape of several reflections and weak intensities on positions not expected for one single domain orientation. Within experimental resolution, the reflections are periodic in the horizontal direction. Additionally, strong diffuse streaks are visible. They are in a periodic alignment in two dimensions according to a period of 5.18 nm enclosing an angle of 72°. The periodic arrangement of the diffuse streaks in reciprocal space indicates a periodic sequence of the net planes being laterally disordered. The orientation of the streaks with regard to the periodic direction of the reflections suggests periodic order related to the cell of the (4,6) approximant.[23] For a perfect (4,6) approximant we should expect sharp reflections at each intersection of streaks according to a C-centered orthorhombic cell with $a=6.1$ nm and $b=8.4$ nm. Figure 3(d) shows a comparison between the observed diffraction pattern and the expected reflection positions for a 1D QC (crosses) and a (4,6) approximant (circles). It is not possible to decide which structure shows a better fit since the expected reflection positions are very close to each other and experimental reflections are quite blurred and elongated.

Annealing of the preannealed sample at 1140 K for 2718 h reveals a normal crystalline phase. A diffraction pattern of the X phase in [010]-direction is presented in Fig. 4(e). The decagonal phase shown in Fig. 4(a) shows sharp reflections of the basic decagonal phase and weak diffuse reflections at positions expected for the S1 superstructure as shown in Fig. 4(c). However, diffraction patterns with weak reflections typical for SST-II are also observed [Figs. 4(b),(d)]. This suggests that the transition was not completed even after annealing for 2718 h.

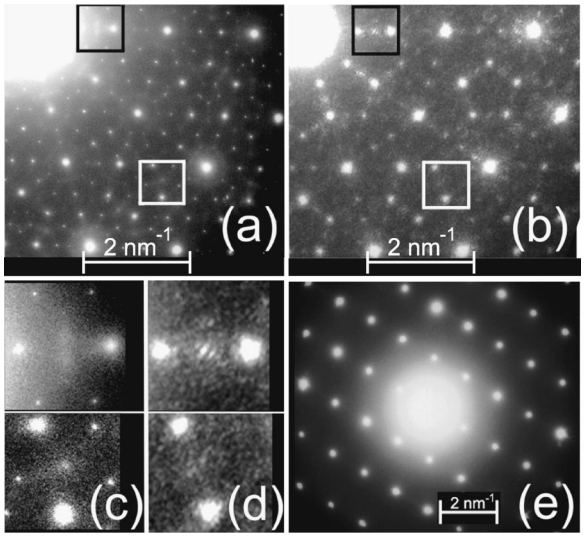

FIG. 4. Diffraction patterns of decomposed material annealed for 2718 h at 1140 K. (a) Decagonal quasicrystal exhibiting reflections of the basic decagonal phase. Diffuse reflections at positions expected for the S1 superstructure emerge; see the magnified details in (c). A residual transition state with weak SST-II reflections is shown in (b). (d) Magnified details of (b). The crystalline *X* phase in the [010] direction is shown in (e).

V. ANALYSIS OF THE HRTEM IMAGES

In Sec. V A we recall some fundamental properties of quasicrystallography. For a more detailed description, see, for example Yamamoto.[30] Readers familiar with the concepts of phason strain may skip to Sec. V B. Here the principles of evaluation by HRTEM with focus on the problems treated in this paper are discussed. In Sec. V C experimental HRTEM micrographs are evaluated.

A. Phason strain

Tilings from HRTEM images and electron diffraction patterns taken with small apertures can give local information on phason strain of single domains. Phason strain is a measure for the deviation of a tiling from ideal quasicrystalline order. The relationship between two-dimensional quasicrystals, approximants, and 1D QC's can be described in terms of phason strain[31] where approximants and 1D QC's correspond to special values of linear phason strain with respect to a two-dimensional quasicrystal.

Each vertex of a decagonal tiling with edge length a can be indexed unambigiously as linear combinations of four vectors $\mathbf{e}_i = a(\cos(2\pi i/5), \sin(2\pi i/5))$, $i=1,\ldots,4$, resulting in the coordinates $\mathbf{r}_\parallel = \Sigma_i n_i \mathbf{e}_i$, where n_i are integers. The vectors $\mathbf{e}_i$ can be regarded as projections of a basis of a four-dimensional lattice. This four-dimensional space can be divided into physical space (tiling) and perpendicular space with $\mathbf{r}_\perp = \Sigma_i n_i \mathbf{e}_{2i}$. The projection of all vertices of an ideal quasiperiodic tiling into perpendicular space (perpendicular projection) must lie within so called acceptance domains[32] A_p, i.e., $\{\mathbf{r}_\perp\} \subset A_p$, which can be different depending on $p = (\Sigma_i n_i)_{\mathrm{mod}\,5}$. The type of the quasiperiodic tiling determines size and shape of the acceptance domains. If a tiling deviates from ideal quasiperiodicity there are also projected vertices outside of the acceptance domain. Statistical deviations from quasiperiodicity leading to an isotropic distribution of projected vertices are random phason fluctuations (around the average phason strain $\mathbf{E}=\mathbf{0}$). In the case of linear phason strain, the distribution of vertices in perpendicular space is anisotropic. $\mathbf{E}$ is then given by a 2×2 matrix in the case of a two-dimensional quasicrystal. For an infinite extension of a tiling with linear phason strain, the projection of the vertices extends infinitely in perpendicular space. An interesting method to analyze linear phason strain in experimental tilings using an inclined projection of vertices is described by Ritsch *et al.*[24] By this method the vertices can be reprojected into the acceptance domain by applying a reverse transformation corresponding to the present or expected linear phason strain: $\mathbf{r}_{\mathrm{incl}} = \mathbf{r}_\perp - \mathbf{E}\mathbf{r}_\parallel$. By this means one can check if a tiling shows a certain value of linear phason strain. In the diffraction pattern linear phason strain causes peak shifts.[33] Thus $\mathbf{E}$ can be determined according to $\mathbf{k}_\parallel = \mathbf{k}_{\mathrm{id}} + \mathbf{E}^\dagger \mathbf{k}_\perp$, where $\mathbf{k}_{\mathrm{id}}$ is the peak position of an ideal quasicrystal which is shifted by the transpose of $\mathbf{E}$ to the measured peak position $\mathbf{k}_\parallel$.

B. Principles of tiling evaluation

The evaluation of the HRTEM images is based on the presumtion that tilings from HRTEM images reflect the underlying structure. This presumption is supported by the fact that for different structures recorded by electron diffraction typical tilings were observed.

To understand the occurrence of ordering states and their eventual stability, we have to look carefully at their transformation behavior. One possibility is to verify the amount of phason strain for a series of annealing treatments at the same temperature for different annealing times. This gives information about tendencies of a transformation if the transition is incomplete. However, it should always be kept in mind that phason strain might have been introduced on quenching the sample. Phason strain values are given with respect to the tiling experimentally observed in the HRTEM images as distances of building units (edge length 2 nm). In this description the lattice of the (4,6) approximant is given by integer multiples of the coordinates $(1,0,-2,-2)$ and $(-1,-2,-2,0)$. For the (4,6) approximant this results in the following elements for $\mathbf{E}$: $\epsilon_{11}=0.0557$, $\epsilon_{22}=0.2361$, and $\epsilon_{21}=\epsilon_{12}=0$. For the C-centered 1D QC with $a=6.1$ nm, $\epsilon_{22}=0.2361$ and $\epsilon_{11}=\epsilon_{12}=\epsilon_{21}=0$. Figures 5(a) and 5(c) show the resulting tilings with an acceptance domain of a Penrose pentagon tiling (PPT). Inclined projections are shown according to the respective phason strain matrices in Figs. 5(b) and 5(d). The small value for ϵ_{11} in the phason strain matrix of the (4,6) approximant as well as the local similarity of the 1D QC and the (4,6) approximant expresses the close relationship between these structures. The tiling of the (4,6) approximant derived from a PPT contains only pentagons, thin rhombi, and thick rhombi. Changing the size or the shape of the acceptance domains changes also the vertex density and the type of occurring motifs. If we want to compare the derived (4,6) approximant with experimental tilings, the choice of

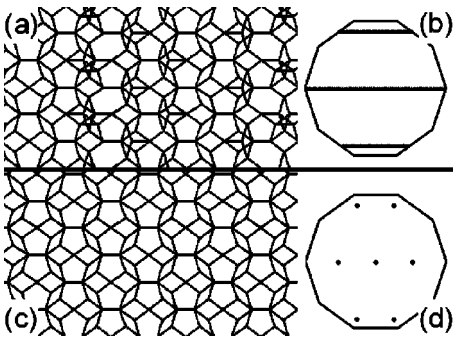

FIG. 5. Tilings of a (a) 1D QC and (c) the (4,6) approximant derived from a Penrose pentagon tiling, and (b),(d) the inclined projections according to their respective phason strain.

the acceptance domains should be justified by the occurrence of the same motifs. Practically, the identification of vertices on a HRTEM micrograph depends on the defocus value and the thickness of the sample. On the micrograph shown in Fig. 6(a), wheel-like features with a bright pentagon in the middle are used as vertices to construct a tiling [Fig. 6(b)]. With increasing thickness [lower part of Fig. 6(a)] the contrast of this structural unit changes to a large white dot surrounded by dark dots. This image was recorded around the Scherzer defocus (-64 nm) as is the case for the other HRTEM images used in this publication. When large regions are recorded the defocus changes considerably if the grain surface under investigation is not perpendicluar to the electron beam. As a consequence, there are also evaluated regions being not in the Scherzer defocus. However, in this study the vertices in a distance of 2 nm are always recognizable by a strong pseudofivefold contrast around the centers. Systematic changes in the tiling were also not observed with the change of the thickness of a sample.[45]

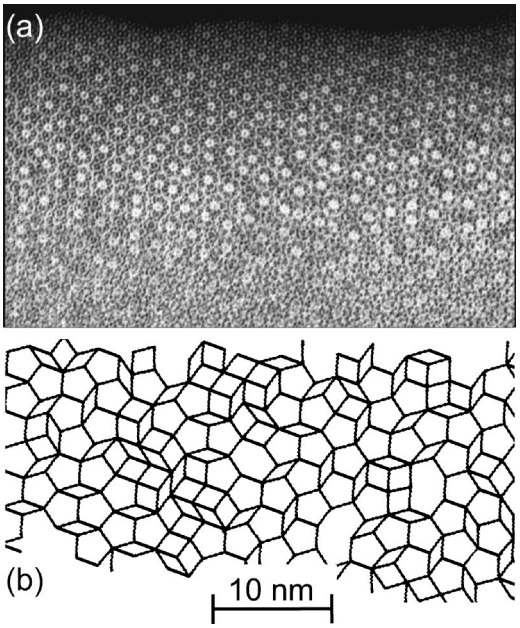

FIG. 6. (a) HRTEM image and (b) the corresponding tiling of material annealed for 384 h at 1140 K taken at the sample position of diffraction pattern from Fig. 1(c).

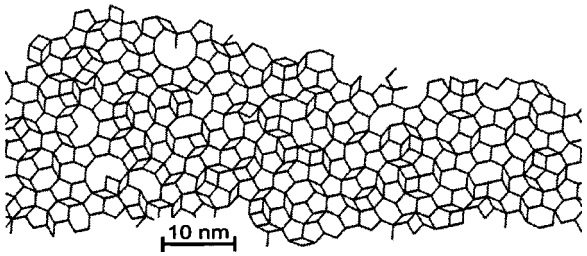

FIG. 7. Tiling of the material preannealed at 1290 K for 43 h corresponding to the diffraction pattern of Fig. 1(a).

C. Evaluation of tilings

The tiling of a HRTEM image of the material preannealed at 1290 K [compare the corresponding diffraction pattern from Fig. 1(a)] is presented in Fig. 7. It is made up by pentagons to a considerable part and a variety of other motifs. The perpendicular projection of the tiling is shown in Fig. 8(a). The great majority of vertices fits into the decagonal acceptance domains of the basic decagonal phase. For comparison, one of the large pentagonal acceptance domains of a Penrose tiling corresponding to the S1 and S2 superstructures is presented. Annealing for 384 h at 1140 K generally results in an increase of phason strain and in a change of the tiling. However, it significantly varies for the different transformation stages revealed by electron diffraction. The perpendicular projection of the tiling from Fig. 6(b) that corresponds to the diffraction pattern of Fig. 1(c) is shown in Fig. 8(b). At first sight it suggests a random character of the phason strain. However, by subdividing the tiling into smaller parts we observe an anisotropic distribution of vertices in perpendicular space indicating linear phason strain for the subtilings [Fig. 8(c)]. Comparing the tilings of Fig. 7 to Fig. 6(b) we observe that the number of pentagons has decreased. The tiling of Fig. 6(b) roughly consists now of pentagons and thin and thick rhombi to equal parts.

The corresponding tiling of a part of a HRTEM micrograph recorded exactly at the same sample position as the diffraction pattern of Fig. 2 is shown in Fig. 9. The tiling is built mainly from pentagons and thin and thick rhombi. A tiling analysis reveals two domains of a 1D QC in the same orientation. This is illustrated by the parallel net planes in a

FIG. 8. (a) Perpendicular projection of the tiling from Fig. 7. For comparison, a large acceptance domain of the Penrose tiling (pentagon) and the acceptance domain of the basic decagonal phase (decagon) is shown. (b) Perpendicular projection corresponding to diffraction pattern of Fig. 1(c) and the tiling of Fig. 6(b). In the perpendicular projection a much larger region is evaluated than shown in the tiling of Fig. 6(b). (c) Perpendicular projection of a subtiling of a smaller ''domain'' from Fig. 6(b) showing an anisotropic distribution of vertices.

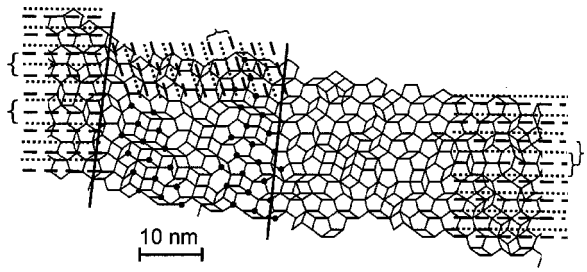

FIG. 9. Tiling of a HRTEM image taken exactly from a sample position where the diffraction pattern of Fig. 2 was observed. The solid lines indicate the rough position of domain boundaries. The evaluated part of the left domain is much larger than indicated by this detail image. Dashed and dotted lines indicate the periodic arrangement of net planes, and brackets indicate deviations from periodicity. Large dots correspond to periodic vertices within net planes ($d=3.05$ nm).

distance of 3.05 nm drawn in the tiling. The translation in the periodic direction corresponds to a distance of 6.1 nm according to the C centering of the 1D QC.[11,23] Most of the building units are located on these net planes but there is only a subset of building units in a periodic relationship of 6.1 nm. In addition, the sequence of net planes is only locally periodic. Therefore the 1D QC has to be considered as rather imperfect. The two domains in the same orientation are separated by a small domain in the middle whose orientation is tilted by 72° with respect to the other domains. The streaks observed in the diffraction pattern stem from this region as a fast Fourier transform of a HRTEM micrograph taken from this region shows. The perpendicular projection of the tiling in Fig. 9 has a large anisotropic extension in perpendicular space as can be seen in Fig. 10(a). As suggested by the diffraction pattern from Fig. 2 an inclined projection according to a 1D QC for the respective orientations is shown for the three domains in Figs. 10(b)–10(d). The vertical extension is a measure for the periodicity of the net planes while the horizontal extension illustrates the deviation from quasiperiodicity within the net planes. The inclined projections of the

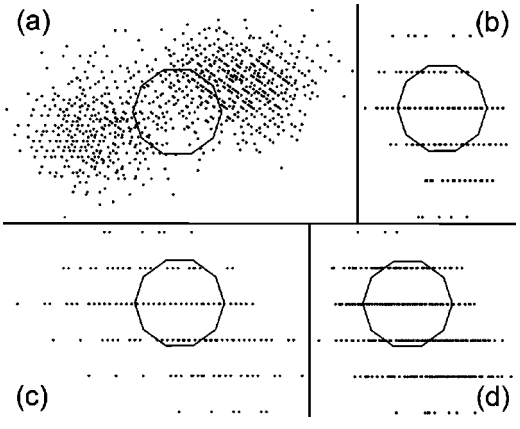

FIG. 10. (a) Perpendicular projection of the tiling from Fig. 9 (annealed for 384 h at 1140 K). (b)–(d) Inclined projections of the three domains of the tiling from Fig. 9 according to a 1D QC . The orientation of (c), corresponding to the domain in the middle of Fig. 9, is tilted by 72° with respect to (b) and (d).

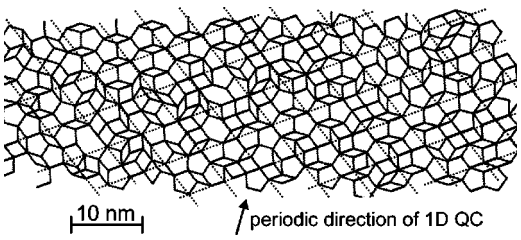

FIG. 11. Tiling from a HRTEM image taken at the sample position of diffraction pattern from Fig. 3(c). Dotted lines indicate strongly occupied net planes forming the lattice of the (4,6) approximant.

domains reflect the basic order of a 1D QC as well as considerable deviations from it. Within the periodically arranged net planes the domain in the middle deviates strongly from quasiperiodic order to periodic short range order ($d=3.05$ nm) indicated by dots in Fig. 9.

A HRTEM image originating from material annealed for 1125 h at 1140 K is shown in Fig. 11(a). It is taken exactly from the same region as the diffraction pattern of Fig. 3(c). As the reflection positions indicate a 1D QC or a (4,6) approximant we would expect a periodic arrangement of vertices. However, periodic order in the tiling is not observed at first sight. The tiling is built of pentagons and thin and thick rhombi. A close inspection reveals that there are parallel equidistant planes strongly occupied by building units extending over almost the whole image [Fig. 11(a)]. The resulting lattice corresponds to the (4,6) approximant in the monoclinic setting: ($a=b=5.18$ nm, $\gamma=108°$). Additionally, there is a subset of vertices in a periodic arrangement with respect to this lattice. For example, most of the lattice points are occupied by vertices. Note that the parallel net planes are extended roughly perpendicular to the periodic direction according to a 1D QC. The lateral occupation of net planes is not completely periodic but shows some disorder. The observation of periodic order in the HRTEM images of the material annealed for 1125 h at 1140 K is in principle not very astonishing. For example, a 1D QC also shows a periodic substructure for small domain sizes as can be seen on Fig. 5, where a 1D QC derived from a PPT is shown. Apart from the ideal periodicity in the vertical direction the local periodicity in the horizontal direction is clearly visible. It is well known that a quasiperiodic sequence also contains limited areas of periodic sequences. However, the periodic streaks in the diffraction pattern suggest that the periodic order allowed for a 1D QC is somehow exceeded. This is the case if the horizontal extension of a projection of the *periodic* vertices according to the inclined projection of a 1D QC is larger than the corresponding acceptance domain. This means for the tiling that the periodic domain must exceed a certain size in the direction perpendicular to the periodic direction of the 1D QC. The size depends on the number of periodically arranged vertices of a cell. In the limit of a completely periodic arrangement of vertices only a few unit cells are needed to exceed the periodic order allowed for a 1D QC. The perpendicular projection of the prevailing domain of the tiling from Fig. 11 is presented in Fig. 12(a). In Fig. 12(b) its inclined projection according to a 1D QC is shown. Although

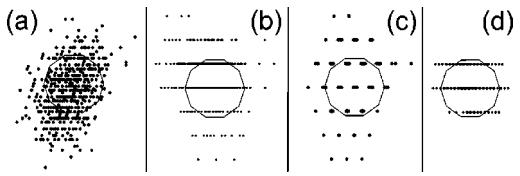

FIG. 12. (a) Perpendicular projection of the tiling from Fig. 11(b) (annealed for 1125 h at 1140 K after preannealing). (b) and (c) show an inclined projection of the prevailing domain according to a 1D QC and the (4,6) approximant, respectively. To demonstrate the number of projected vertices on a projection point the projection angle in (c) slightly deviates from the theoretical value. The periodic substructure that corresponds to the simulated cell of the (4,6) approximant in an inclined projection according to a 1D QC is shown in (d).

the horizontal and the vertical extension exceeds the acceptance domain by far it can be seen that the highest vertex density is in a narrow region on only four lines. This shows that the order present can be described at least coarsely to be one-dimensional quasicrystalline. The projection angle according to a the (4,6) approximant in Fig. 12(c) has been slightly modified to illustrate the number of vertices projected onto the each point. In Fig. 12(d) the inclined projection according to a 1D QC of the periodic substructure that corresponds to the simulated cell of the (4,6) approximant [Fig. 5(b)] is shown. It clearly exceeds the acceptance domain of the 1D QC. Despite the existence of disorder that should rather shrink the periodic domain, the periodic order exceeds that allowed for a 1D QC. The choice of the vertices of the cell from the simulated (4,6) approximant is somehow arbitrary because we do not have an indication that the material finally transforms in this structure. Indeed, there exist other periodic subsets of the experimental structure with larger extensions of the inclined projections according to a 1D QC. However, for means of comparability between evaluated tilings we stick to the simulated cell of the (4,6) approximant. It should be stressed that truly periodic domains and a defined unit cell were never observed in this study.

The diffraction pattern of the quasicrystal shown in Fig. 4(b) observed after annealing 2718 h at 1140 K indicates

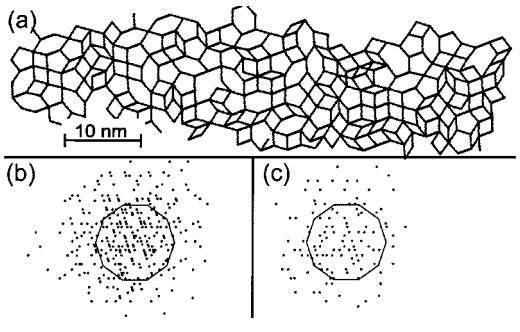

FIG. 13. (a) Tiling of a HRTEM image corresponding to the diffraction pattern of Fig. 4(b). (b) Perpendicular projection of all vertices of (a). (c) shows the perpendicular projection of a subtiling, the right quarter of (a). In this case, the anisotropic distribution of vertices is not as clear as in Fig. 8(c) .

strong disorder. In the corresponding tiling from Fig. 13(a), the number of pentagons has decreased significantly at the cost of hexagons and thick rhombi. These motifs are typical for the S2-superstructure.[34,4] However, the corresponding S1 and S2 reflections are not observed besides the weak SST-II reflecions. The perpendicular projection of the tiling shows an isotropic distribution of vertices and a rather large extension in perpendicular space [Fig. 13(b)]. In comparision to Figs. 8(b) and 8(c), the distribution of projected vertices seems to be less anisotropic when we divide the tiling into smaller subtilings as is shown in Fig. 13(c).

VI. DISCUSSION

A. Sequence and stability of structures

The sequence of transition states observed in the preannealed samples with subsequent annealing at 1140 K obviously corresponds to an increase of linear phason strain. The sample that was only preannealed does not show linear phason strain. This suggests that at this composition no transition from quasiperiodic to periodic occurs during quenching also at lower temperatures because of the confined mobility of atoms at lower temperatures. All diffraction patterns of the preannealed sample exhibit S1-superstructure reflections. However, the basic decagonal phase should be stable at temperatures close to the solidus. The pentagons observed in the tiling of the preannealed sample (Fig. 7) are, due to different acceptance domains, rather typical for the basic decagonal phase[34] than for the S1 superstructure. The material is therefore expected to transform partly to the S1 superstructure while passing through its stability region during quenching.

At the beginning of the transition from the S1-superstructure to SST-II the distribution of projected vertices looks rather random. This can be interpreted as a consequence of linear phason strain of very small domains in different orientations plus disorder. In further progression of the transition, the present order can be described coarsely as one-dimensional quasiperiodic. However, by looking at the details of diffraction patterns and tilings, we always observed considerable deviations from a 1D QC signifying that there is no ''lock in'' to a 1D QC. In the case of the two dimensional periodic substructure the order present even exceeds the order required for a 1D QC. A twinning of all these ordering states can produce the diffraction pattern of SST-II. SST-II should therefore be considered as a diffraction pattern resulting from twinned nanodomains roughly with the order of a 1D QC. These ordering states are only metastable as further annealing shows. It is astonishing that after 1125 h annealing, the *X* phase is only a minor phase while after 2718 h considerable amounts of the material are crystalline.

The tiling as well as the composition of the quasicrystal observed after 2718 h suggest that the S2 superstructure is stable at this temperature besides the *X* phase. In the corresponding diffraction patterns the S2 reflections are absent, which possibly signifies the lack of coherence related to the transformation, which is not finished even after 2718 h of annealing. Anyway, the weak SST-II reflections in Fig. 4(b) as well as the absence of SST-II reflections and the appearance of diffuse S1 reflections in Fig. 4(a) point to the forma-

tion of the S1 or the S2 superstructure. The consequences of the decomposition reaction for the phase diagram of Al-Co-Ni will be discussed in a future presentation.

B. Mechanism of stabilization and transformation

In previous studies annealing at similar compositions resulted in the formation of low-temperature ordering states that were suggested to be stable.[4] A phason strain analysis of this material led to the conclusion of a random character of the tilings.[13] We monitored phason strain as a function of annealing time. In our case the phason strain observed cannot be related to the random tiling scenario because the ordering states in question are metastable as shown by the final decomposition. If disorder is present in tilings it might be related, apart from the random tiling hypothesis, to thermodynamic imbalance or distortions introduced by the quenching process. Geometrical disorder could be introduced, for example, by local chemical ordering in the process of phase transformations. In the Ni-rich part of the phase diagram the basic decagonal phase used for many structural models[35–37] can be quenched in as a quasicrystal with a high degree of perfection[38] almost free from random phason strain observable by HRTEM. This might be based on the finding that the quasicrystal at this composition does not show stable or metastable low-temperature quasicrystals or related structures without previous decomposition.[38,39] We have a similar situation in the Al-Ni-Fe system[40,41] at similar Al and Ni contents.

The growth of the 1D QC is characterized by the formation of building units according to a periodicity of 6.1 nm. Forced by centering there is additionally at least one identical building block in a distance of 5.18 nm in an angle of 54° or $-54°$ relating to the periodic direction (compare Fig. 5). In most of the cases building units in both directions can be found. If we require that both positions are occupied in all cases the (4,6) approximant results. Thus, the two-dimensional periodic substructure seems to be a consequence of the same ordering principle as the 1D QC. Furthermore, its occurrence also at different compositions and other material systems suggests that it might be a frequent feature of transitions of decagonal quasicrystals when certain conditions are given. The existence of the (4,6) approximant has always been shown either by high-resolution x-ray diffraction[10,42] or by lattice fringe images.[43] However, to the knowledge of the authors HRTEM images of a completely periodic (4,6) approximant have never been reported. Possibly, a strictly periodic (4,6) approximant does not exist in the systems Al-Ni-Co and Al-Cu-Co. The transition seems to be stuck somewhere between a decagonal quasicrystal and a 1D QC with a two-dimensional periodic substructure, at which point the transition stops might be a function of temperature and composition.

It was frequently observed that quasicrystals did not transform into approximants at low temperatures if they were preannealed at high temperatures.[9,12] It was suggested that metastable vacancies are responsible for the formation of vacancy ordered approximants,[9,12] being consequently also metastable. In previous studies, the formation of twinned NDS's was observed simply by cooling from the melt[10,11] at the composition $Al_{70}Co_{15}Ni_{15}$. The drastic difference of the transformation kinetics as compared to our results therefore is expected to be related to our preannealing of the material at high temperatures by which defects can be healed out. Thus preannealing obstructs the formation of (more) stable phases. From the experimental point of view we are in a difficult situation: Healing out defects can obstruct the transformation thus requiring extremely long annealing times, quenched-in defects can produce metastable phases.

For the transition between decagonal quasicrystals and approximants it was predicted by Steurer[44] that in one of the first steps of the transition the periodic domains show a disordered structure because of the lack of diffusion at this stage of the transition. Only if diffusion takes place can the resulting structure become strictly periodic. Our observations could be described by a basic periodic structure plus disorder. A periodic substructure might be the maximum periodic order possible if only small atomic displacements can occur. Diffusion sets in after supercritical seeds of other phases are formed, which might be the critical step concerning the transition kinetics towards stable phases. Otherwise we would not observe metastable NDS's even after 1125 h annealing duration as a major ordering state. Simulations for displacements of atoms at the transition between a decagonal quasicrystal and a (4,6) approximant were performed by Honal *et al.*[26] In a model where atomic species are not distinguished, more than 95% of atomic shifts are smaller than 0.1 nm. It was stated in this study that a chemically ordered (4,6) approximant requires diffusion. As the transformation to the (4,6) approximant is incomplete, we expect that chemical ordering is one of the main characteristics of this transformation. However, if the first steps of the transition would include only small atomic displacements, we should expect a rather fast transformation from the S1 superstructure to NDS's. The transformation kinetics might indicate more complicated processes promoted by defects even in the first steps of the transition. Another explanation for the slow transformation kinetics from the S1 superstructure to NDS's might be related to the annealing temperature used in this study. Possibly at slightly higher temperatures just below the temperature where the S1 superstructure becomes metastable, the transformation to NDS's is much faster.

ACKNOWLEDGMENTS

We thank V. Zibat for the microprobe analysis. We would like to thank D. Gerthsen, E. Weidner, and F. Frey for inspiring discussions. This investigation was financially supported by the Deutsche Forschungsgemeinschaft under Contract No. Wi1645/1.

*Present address: Robert Bosch GmbH, K3/EVT2, Postfach 300240, D-70442 Stuttgart, Germany.
[1] K. Edagawa, H. Tamaru, S. Yamaguchi, K. Suzuki, and S. Takeuchi, Phys. Rev. B **50**, 12 413 (1994).
[2] B. Grushko and K. Urban, Philos. Mag. B **70**, 1063 (1994).
[3] A. Tsai, A. Fujiwara, A. Inoue, and T. Masumoto, Philos. Mag. Lett. **74**, 233 (1996).
[4] S. Ritsch, Ph.D. thesis, ETH Zürich, 1996.
[5] A. Baumgarte, J. Schreuer, M. Estermann, and W. Steurer, Philos. Mag. A **75**, 1665 (1997).
[6] S. Ritsch, C. Beeli, H.-U. Nissen, T. Gödecke, M. Scheffer, and R. Lück, Philos. Mag. Lett. **78**, 67 (1998).
[7] B. Grushko and D. Holland-Moritz, J. Alloys Compd. **262-263**, 350 (1997).
[8] K. Edagawa, M. Ichihara, K. Suzuki, and S. Takeuchi, Philos. Mag. Lett. **66**, 19 (1992); **66**, 217(E) (1992).
[9] B. Grushko, D. Holland-Moritz, R. Wittmann, and G. Wilde, J. Alloys Compd. **280**, 215 (1998).
[10] M. Kalning, S. Kek, B. Burandt, W. Press, and W. Steurer, J. Phys.: Condens. Matter **6**, 6177 (1994).
[11] M. Kalning, S. Kek, H. Krane, V. Dorna, W. Press, and W. Steurer, Phys. Rev. B **55**, 187 (1997).
[12] S. Ritsch, K. Hiraga, T. Gödecke, and R. Lück, in *Proceedings of the International Conference on Solid–Solid Phase Transitions* edited by M. Koiwa, K. Otsuka, and T. Miyazaki (The Japan Institute of Metals, Kyoto, 1999), pp. 1341–1344.
[13] D. Joseph, S. Ritsch, and C. Beeli, Phys. Rev. B **55**, 8175 (1997).
[14] R. Hory, C. Pohla, and P. Ryder, Philos. Mag. A **79**, 549 (1999).
[15] V. Elser, Phys. Rev. Lett. **54**, 1730 (1985).
[16] C. Henley, V. Elser, and M. Mihalkovič, Z. Kristallogr. **215**, 553 (2000).
[17] C. Henley, in *Quasicrystals: The State of the Art*, edited by D. DiVincenzo and P. Steinhardt (World Scientific, Singapore, 1991), pp. 429–524.
[18] S. Ritsch, H.-U. Nissen, and C. Beeli, Phys. Rev. Lett. **76**, 2507 (1996).
[19] K. Ishihara and A. Yamamoto, Acta Crystallogr., Sect. A: Found. Crystallogr. **44**, 508 (1988).
[20] T. Haibach, A. Cervellino, M. Estermann, and W. Steurer, Philos. Mag. A **79**, 933 (1999).
[21] S. Ritsch, C. Beeli, H.-U. Nissen, and R. Lück, Philos. Mag. A **71**, 671 (1995).
[22] M. Scheffer, Ph.D. thesis, Institut für Metallkunde der Universität und Max-Planck-Institut für Metallforschung, 1998.
[23] K. Edagawa, K. Suzuki, M. Ichihara, S. Takeuchi, and T. Shibuya, Philos. Mag. B **64**, 629 (1991).
[24] S. Ritsch, O. Radulescu, C. Beeli, D. Warrington, R. Lück, and K. Hiraga, Philos. Mag. Lett. **80**, 107 (2000).
[25] E. Weidner, F. Frey, and K. Hradil, Philos. Mag. A (to be published).
[26] M. Honal, T. Haibach, and W. Steurer, Acta Crystallogr., Sect. A: Found. Crystallogr. **54**, 374 (1998).
[27] W. Steurer and F. Frey, Phase Transit. **67**, 319 (1998).
[28] R. Wittmann, M. Fettweis, P. Launois, R. Reich, and F. Dénoyer, Philos. Mag. Lett. **71**, 147 (1995).
[29] T. Gödecke, M. Scheffer, R. Lück, S. Ritsch, and C. Beeli, Z. Metallkd. **89**, 687 (1998).
[30] A. Yamamoto, Acta Crystallogr., Sect. A: Found. Crystallogr. **52**, 509 (1996).
[31] H. Zhang and K. Kuo, Phys. Rev. B **41**, 3482 (1990).
[32] T. Janssen, Acta Crystallogr., Sect. A: Found. Crystallogr. **42**, 261 (1986).
[33] T. Lubensky, J. Socolar, P. Steinhardt, P. Bancel, and P. Heiney, Phys. Rev. Lett. **57**, 1440 (1986).
[34] K. Hiraga, W. Sun, and A. Yamamoto, Mater. Trans., JIM **35**, 657 (1994).
[35] P. Steinhardt, H.-C. Jeong, K. Saitoh, M. Tanaka, E. Abe, and A. Tsai, Nature (London) **396**, 55 (1998).
[36] Y. Yan, S. Pennycook, and A. Tsai, Phys. Rev. Lett. **81**, 5145 (1998).
[37] K. Saitoh, K. Tsuda, and M. Tanaka, J. Phys. Soc. Jpn. **67**, 2578 (1998).
[38] S. Ritsch, C. Beeli, H.-U. Nissen, T. Gödecke, M. Scheffer, and R. Lück, Philos. Mag. Lett. **74**, 99 (1996).
[39] B. Grushko and D. Holland-Moritz, Scr. Mater. **35**, 1141 (1996).
[40] K. Hiraga, K. Yubuta, and K.-T. Park, J. Mater. Res. **11**, 1702 (1996).
[41] B. Grushko, U. Lemmerz, K. Fischer, and C. Freiburg, Phys. Status Solidi A **155**, 17 (1996).
[42] M. Fettweis, P. Launois, F. Dénoyer, R. Reich, and M. Lambert, Phys. Rev. B **49**, 15573 (1994).
[43] S. Song, L. Wang, and E. Ryba, J. Mater. Sci. Lett. **12**, 80 (1993).
[44] W. Steurer, in *Quasicrystals*, edited by J. M. Dubois, P. A. Thiel, A. P. Tsai, and K. Urban, MRS Symposia Proceedings No. 553 (Materials Research Society, Pittsburgh, 1999), p. 159.
[45] HRTEM images used for constructing the tilings can be downloaded at www.quasicrystals.org